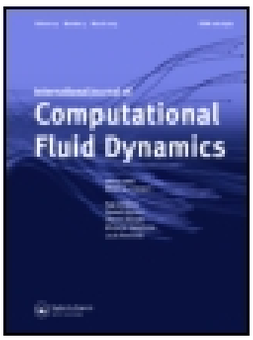

International Journal of Computational Fluid Dynamics

ISSN: 1061-8562 (Print) 1029-0257 (Online) Journal homepage: http://www.tandfonline.com/loi/gcfd20

All-speed Roe scheme for the large eddy simulation of homogeneous decaying turbulence

Xue-song Li & Xin-liang Li

To cite this article: Xue-song Li & Xin-liang Li (2016): All-speed Roe scheme for the large eddy simulation of homogeneous decaying turbulence, International Journal of Computational Fluid Dynamics

To link to this article: http://dx.doi.org/10.1080/10618562.2016.1156095

Published online: 17 Mar 2016.

INTERNATIONAL JOURNAL OF COMPUTATIONAL FLUID DYNAMICS, 2016
http://dx.doi.org/10.1080/10618562.2016.1156095

Taylor & Francis
Taylor & Francis Group

All-speed Roe scheme for the large eddy simulation of homogeneous decaying turbulence

Xue-song Li[a] and Xin-liang Li[b]

[a]Key Laboratory for Thermal Science and Power Engineering of Ministry of Education, Department of Thermal Engineering, Tsinghua University, Beijing, China; [b]The State Key Laboratory of High-temperature Gas Dynamics (LHD), Institute of Mechanics, Chinese Academy of Sciences, Beijing, China

ABSTRACT

As a type of shock-capturing scheme, the traditional Roe scheme fails in large eddy simulation (LES) because it cannot reproduce important turbulent characteristics, such as the famous $k^{-5/3}$ spectral law, as a consequence of the large numerical dissipation. In this work, the Roe scheme is divided into five parts, namely, ξ, δU_p, δp_p, δU_u, and δp_u, which denote basic upwind dissipation, pressure difference-driven modification of interface fluxes, pressure difference-driven modification of pressure, velocity difference-driven modification of interface fluxes, and velocity difference-driven modification of pressure, respectively. Then, the role of each part in the LES of homogeneous decaying turbulence with a low Mach number is investigated. Results show that the parts δU_u, δp_p, and δU_p have little effect on LES. Such minimal effect is integral to computational stability, especially for δU_p. The large numerical dissipation is due to ξ and δp_u, each of which features a larger dissipation than the sub-grid scale model. On the basis of these conditions, an improved all-speed Roe scheme for LES is proposed. This scheme can provide satisfactory LES results even for coarse grid resolutions with usually adopted second-order reconstructions for the finite volume method.

ARTICLE HISTORY
Received 5 November 2015
Accepted 14 February 2016

KEYWORDS
Roe scheme; all-speed scheme; large eddy simulation; homogeneous decaying turbulence; numerical dissipation

1. Introduction

Large eddy simulation (LES) has become increasingly important in the unsteady turbulence computation of incompressible and compressible flows. It achieves satisfactory development, especially for incompressible flows. As one of the most important achievements of computational fluid dynamics (CFD), the shock-capturing scheme is generally adopted for compressible flow computation. Therefore, the role of intrinsic numerical dissipation in the shock-capturing scheme needs to be identified for LES.

In recent years there are several state-of the-art articles for the error analyses of implicit LES computations with shock-capturing schemes, such as the monograph of Grinstein, Margolin, and Rider (2007), and journal papers of San and Kara (2014, 2015), which address dissipation mechanism of shock-capturing schemes for two-dimensional decaying turbulence characteristics. The classical Roe scheme, as one of the most popular shock-capturing schemes, has also been investigated for the LES of homogeneous decaying turbulence (HDT) with a low Mach number (Garnier et al. 1999; Thornber, Mosedale, and Drikakis 2007). However, the result of this scheme is disappointing because it cannot reproduce many important turbulent characteristics. For example, the popular $k^{-5/3}$ spectral sub-ranges in the self-similar decay stage of the Roe scheme for LES can only be produced in a very narrow range of wave numbers. In fact, in a range of high wave numbers, the numerical slope of the kinetic energy spectrum reaches approximately –5, which is significantly greater than –5/3 of all the schemes (Garnier et al. 1999; Thornber, Mosedale, and Drikakis 2007), including the fifth-order (Garnier et al. 1999) and ninth-order (Thornber, Mosedale, and Drikakis 2007) schemes. Such difference indicates that the physical sub-grid scale (SGS) dissipation is fully immersed by the numerical dissipation and cannot satisfy one of the following conditions for a scheme for LES (Garnier et al. 1999):

(1) Numerical dissipation is significantly lower than physical SGS dissipation (condition (C1)).
(2) Numerical dissipation is able to mimic the features of an SGS model (condition (C2)).

Notably, the shock-capturing scheme itself cannot be directly used for incompressible flow not only in LES but also in the general computation even for Euler flows; its direct use produces unphysical results

CONTACT Xue-song Li xs-li@mail.tsinghua.edu.cn

(Guillard and Viozat 1999; Turkel 1999). The traditional curing method is a preconditioning technology, based on which many improved schemes have been developed; however, schemes such as the preconditioned Roe (Weiss and Smith 1995; Huang 2007), AUSM (Advection Upstream Splitting Method)-type (Liou 2006; Shima and Kitamura 2011), and HLL (Harten -Lax -van Leer)-type (Park, Lee, and Kwon 2006; Luo and Baum 2005) schemes suffer from several limitations. These defects are identified (Li and Gu 2013) as the non-physical behaviour problem, the global cut-off problem, and the checkerboard problem.

The non-physical behaviour problem means that at a low Mach number speed, the physical pressure scales with the square of the Mach number, i.e., $p(\boldsymbol{x}, t) = P_0(t) + M_*^2 p_2(\boldsymbol{x}, t)$; however, the pressure fluctuation solution of the shock-capturing scheme scales with the Mach number, i.e., $p(\boldsymbol{x}, t) = P_0(t) + M_* p_1(\boldsymbol{x}, t)$, where $\boldsymbol{x}$ and t denote space and time, respectively. Therefore, the direct use of the shock-capturing scheme for LES is inappropriate.

Under the global cut-off problem, the local Mach number is replaced with the global reference Mach number for almost all improved shock-capturing schemes by the traditional preconditioning technology. The problem limits the accurate simulation of mixed flows with low and high Mach numbers. For example, for a flow region where shock waves coexist with incompressible flows such as the boundary layer, the calculation of the incompressible region cannot benefit from preconditioning because of the global cut-off problem. The process, in turn, suffers from the non-physical behaviour problem. Therefore, the use of the traditional preconditioned scheme for LES is inappropriate.

The checkerboard problem refers to the classical problem of pressure–velocity decoupling, which indicates a pressure solution with checkerboard oscillation for incompressible flows. The scheme for low Mach number flows must feature a mechanism for suppressing the checkerboard problem; otherwise, the computation becomes unstable and divergent. Therefore, the suppression mechanism should also be investigated for LES because it cannot be avoided.

The three problems may all be due to the construction of the numerical dissipation of the scheme; they are addressed on the basis of three general rules (Li and Gu 2013). These rules increase the possibility of obtaining an LES scheme that satisfies condition (C1) or condition (C2) by modifying the shock-capturing scheme. However, according to the general premise of these three general rules, a method that satisfies LES should still be identified. In this work, we investigate the role of each term of the numerical dissipation of the Roe scheme for LES and then propose an improved Roe scheme that satisfies condition (C2).

The outline of this paper is as follows. Section 2 presents the governing equations and the different forms of the Roe scheme. Section 3 discusses the effect of each part of the Roe scheme in LES. Section 4 proposes an improved all-speed Roe scheme for LES that satisfies condition (C2). Finally, Section 5 closes the paper with some concluding remarks.

2. Governing equations and the Roe scheme

2.1. Governing equations

The governing three-dimensional Navier–Stokes equations can be written as follows:

$$\frac{\partial \boldsymbol{Q}}{\partial t} + \frac{\partial \boldsymbol{F}}{\partial x} + \frac{\partial \boldsymbol{G}}{\partial y} + \frac{\partial \boldsymbol{H}}{\partial z} = \frac{\partial \boldsymbol{F^v}}{\partial x} + \frac{\partial \boldsymbol{G^v}}{\partial y} + \frac{\partial \boldsymbol{H^v}}{\partial z}, \quad (1)$$

where $\boldsymbol{Q} = \begin{bmatrix} \rho \\ \rho u \\ \rho v \\ \rho w \\ \rho E \end{bmatrix}$ is the vector of conservation variables; $\boldsymbol{F} = \begin{bmatrix} \rho u \\ \rho u^2 + p \\ \rho uv \\ \rho uw \\ u(\rho E + p) \end{bmatrix}$, $\boldsymbol{G} = \begin{bmatrix} \rho v \\ \rho uv \\ \rho v^2 + p \\ \rho vw \\ v(\rho E + p) \end{bmatrix}$, and $\boldsymbol{H} = \begin{bmatrix} \rho w \\ \rho uw \\ \rho vw \\ \rho w^2 + p \\ w(\rho E + p) \end{bmatrix}$ are the vectors of Euler fluxes; $\boldsymbol{F^v}$, $\boldsymbol{G^v}$, and $\boldsymbol{H^v}$ are the vectors of the viscous fluxes, the details of which are not presented here for simplicity; ρ is fluid density; p is pressure; E is the total energy; and u, v, w are the velocity components in the Cartesian coordinates (x, y, z), respectively.

2.2. Original form of the Roe scheme

The classical Roe scheme can be expressed as the following general sum form of a central term and a numerical dissipation term:

$$\tilde{\boldsymbol{F}} = \tilde{\boldsymbol{F}}_{\boldsymbol{c}} + \tilde{\boldsymbol{F}}_{\boldsymbol{d}}, \quad (2)$$

where $\tilde{\boldsymbol{F}}_{\boldsymbol{c}}$ is the central term and $\tilde{\boldsymbol{F}}_{\boldsymbol{d}}$ is the numerical dissipation term.

$$\tilde{\boldsymbol{F}}_{c,\,1/2} = \frac{1}{2}\left(\bar{\boldsymbol{F}}_L + \bar{\boldsymbol{F}}_R\right), \quad (3)$$

$$\bar{\boldsymbol{F}} = U \begin{bmatrix} \rho \\ \rho u \\ \rho v \\ \rho w \\ \rho H \end{bmatrix} + \begin{bmatrix} 0 \\ n_x p \\ n_y p \\ n_z p \\ 0 \end{bmatrix}, \quad (4)$$

$$\tilde{\boldsymbol{F}}_{d,\,1/2} = -\frac{1}{2}\boldsymbol{R}_{1/2}\boldsymbol{\Lambda}_{1/2}\left(\boldsymbol{R}_{1/2}\right)^{-1}\left(\boldsymbol{Q}_R - \boldsymbol{Q}_L\right), \quad (5)$$

$$\boldsymbol{R} = \begin{bmatrix} n_x & n_y & n_z & 1 & 1 \\ n_x u & n_y u - n_z & n_z u + n_y & u - n_x c & u + n_x c \\ n_x v + n_z & n_y v & n_z v - n_x & v - n_y c & v + n_y c \\ n_x w - n_y & n_y w + n_x & n_z w & w - n_z c & w + n_z c \\ n_z v - n_y w + \frac{V_M^2}{2} n_x & n_x w - n_z u + \frac{V_M^2}{2} n_y & n_y u - n_x v + \frac{V_M^2}{2} n_z & H - cU & H + cU \end{bmatrix}, \quad (6)$$

$$\boldsymbol{\Lambda}^{\mathrm{Roe}} = \begin{bmatrix} |U| & & & & \\ & |U| & & & \\ & & |U| & & \\ & & & |U - c| & \\ & & & & |U + c| \end{bmatrix}, \quad (7)$$

where c is the speed of sound; $V_M^2 = u^2 + v^2 + w^2$; $U = n_x u + n_y v + n_z w$ is the normal velocity on the cell interface; $H$is the total enthalpy; and n_x, n_y, and n_z are the components of the face-normal vector.

2.3. Scalar form of the Roe scheme

Following Weiss and Smith (1995), the numerical dissipation term of the Roe scheme in Section 2.2 can also be rewritten in the following scalar form:

$$\tilde{\boldsymbol{F}}_{\boldsymbol{d}} = -\frac{1}{2}\left\{ \xi \begin{bmatrix} \Delta\rho \\ \Delta(\rho u) \\ \Delta(\rho v) \\ \Delta(\rho w) \\ \Delta(\rho E) \end{bmatrix} + \delta p \begin{bmatrix} 0 \\ n_x \\ n_y \\ n_z \\ U \end{bmatrix} + \delta U \begin{bmatrix} \rho \\ \rho u \\ \rho v \\ \rho w \\ \rho H \end{bmatrix} \right\}. \quad (8)$$

Equation (8) can be regarded as the uniform framework for the shock-capturing scheme (Li 2014), and the three terms on the right side have explicit physical meanings: the first term denotes basic upwind dissipation and can be regarded as low Mach-number Roe scheme for LES (Li, Xu, and Gu 2008), the second term denotes a modification of the interface pressure, and the third term denotes a modification of the interface fluxes. Li (2014) proposes the following equations, which are strictly equal to the vector form in Section 2.2:

$$\xi = |U|, \quad (9)$$

$$\delta p = -\frac{|U - c| - |U + c|}{2} c\beta + \left[|U| - \frac{|U - c| + |U + c|}{2} \right] [U\Delta\rho - \Delta(\rho U)], \quad (10)$$

$$\delta U = \frac{1}{\rho}\left(\frac{|U - c| + |U + c|}{2} - |U| \right)\beta + \frac{|U - c| - |U + c|}{2\rho c} [U\Delta\rho - \Delta(\rho U)], \quad (11)$$

where

$$\beta = \frac{\gamma - 1}{c^2}\left[\frac{V_M^2}{2}\Delta\rho - u\Delta(\rho u) - v\Delta(\rho v) - w\Delta(\rho w) + \Delta(\rho E) \right] \quad (12)$$

and γ is the ratio of the specific heat values.

With the assumption

$$\Delta(\rho\phi) = \rho\Delta\phi + \phi\Delta\rho, \quad (13)$$

where ϕ represents one of the fluid variables, the following equations can be obtained:

$$\beta = \frac{\Delta p}{c^2} \text{ and } U\Delta\rho - \Delta(\rho U) = -\rho\Delta U. \quad (14)$$

Further, the terms δU and δp can be subdivided as the sub-terms driven by pressure difference Δp and velocity difference ΔU.

$$\delta U = \delta U_p + \delta U_u, \quad (15)$$

$$\delta p = \delta p_p + \delta p_u. \quad (16)$$

$$\delta p_p = -\frac{|U - c| - |U + c|}{2}\frac{\Delta p}{c}, \quad (17)$$

$$\delta p_u = -\left[|U| - \frac{|U - c| + |U + c|}{2} \right]\rho\Delta U, \quad (18)$$

$$\delta U_p = \left(\frac{|U - c| + |U + c|}{2} - |U| \right)\frac{\Delta p}{\rho c^2}, \quad (19)$$

$$\delta U_u = -\frac{|U - c| - |U + c|}{2c}\Delta U. \quad (20)$$

That is, δU_p, δU_u and δp_p, δp_u denote the pressure difference-driven and velocity difference-driven modifications on the interface velocity and pressure, respectively.

For the low Mach number flows, Equations (17)–(20) can be simplified as follows:

$$\delta p_p = \frac{U}{c}\Delta p, \tag{21}$$

$$\delta p_u = (c - |U|)\,\rho\Delta U, \tag{22}$$

$$\delta U_p = (c - |U|)\,\frac{\Delta p}{\rho c^2}, \tag{23}$$

$$\delta U_u = \frac{U}{c}\Delta U. \tag{24}$$

As demonstrated by Li (2013, 2014), the non-physical behaviour problem is due to δp_u and the checkerboard problem is due to δU_p. The Roe scheme has an inherent mechanism of suppressing the checkerboard problem because δU_p plays a role similar to that of the momentum interpolation method (Li and Gu 2010); however, it fails to resolve the non-physical behaviour problem because the coefficient of the velocity difference dissipation term ΔU in δp_u is too large with the order of $O(c)$. δU_u and δp_p seem trivial for the low Mach number flows because they have little effect on numerical results (Li and Gu 2013).

The above discussions indicate that the numerical dissipation of the Roe scheme can be divided into five parts, namely, ξ, δU_p, δU_u, δp_p, and δp_u. These parts have different effects on computation and can be modified independently according to specific requirements. This division provides a new way to develop LES schemes. Moreover, this approach is different from the traditional way of increasing the order of schemes and appears to be important, especially under the current condition of the finite volume method in which the traditional high-order approach is difficult to employ in LES (Garnier et al. 1999; Thornber, Mosedale, and Drikakis 2007). Therefore, in the following section, the roles of the five parts in the LES of HDT are investigated.

3. Mechanism of the Roe scheme for the LES of HDT

3.1. Numerical method

To understand the effect of the five parts of the Roe scheme on LES, nine cases are designed and presented in Table 1. In Table 1, the numbers refer to the coefficients of the five parts of the Roe scheme and the Smagorinsky model (denoted as SMA), which is the classical SGS model of LES.

Table 1. Nine cases.

	ξ	δU_p	δU_u	δp_p	δp_u	Smagorinsky model (SMA)
Case 1 (Cen-SMA)	0	0	0	0	0	1
Case 2 (Cen)	0	0	0	0	0	0
Case 3 (Roe)	1	1	1	1	1	0
Case 4 (ξ)	1	0	0	0	0	0
Case 5 (δU_p)	0	1	0	0	0	0
Case 6 (δU_u)	0	0	1	0	0	0
Case 7 (δp_p)	0	0	0	1	0	0
Case 8 (δp_u)	0	0	0	0	1	0
Case 9 (0.5ξ)	0.5	0	0	0	0	0

$$\mu_{\mathrm{SMA}} = \rho C_s^2 \Delta^2 \sqrt{2S_{ij}S_{ij}}, \tag{25}$$

where $S_{ij} = \frac{1}{2}\left(\frac{\partial u_i}{\partial x_j} + \frac{\partial u_j}{\partial x_i}\right)$, the filter width Δ is equal to the cell size, and the Smagorinsky constant C_S is set to 0.2.

Therefore, Case 1 (denoted as Cen-SMA for clarity) entails a normal LES process, in which the SMA and a centre scheme are adopted, i.e.,

$$\tilde{\boldsymbol{F}}_{\boldsymbol{d}} = 0. \tag{26}$$

In Case 2 (denoted as Cen), only the centre scheme without the SGS model is adopted to understand the behaviour of the scheme itself. Case 3 (denoted as Roe) is simply the Roe scheme because of the adoption of all five parts. In Cases 4–8 (denoted as ξ, δU_p, δU_u, δp_p, and δp_u), only one part of the Roe scheme is adopted to investigate the role of each part. To mimic the Smagorinsky model, only ξ with a coefficient of 0.5 is adopted in Case 9 (denoted as 0.5ξ), i.e.,

$$\tilde{\boldsymbol{F}}_{\boldsymbol{d}} = 0.5\zeta\,\Delta\boldsymbol{Q} = 0.5\,|U|\,\Delta\boldsymbol{Q}, \tag{27}$$

which represents only half of the numerical dissipation of the common basic upwind dissipation in this case.

For the high-order accuracy of space discretisation, there are many reconstruction methods such as the monotone upstream-centred schemes for conservation laws (MUSCL) (Van Leer 1979; Leng et al. 2012), the weighted essentially nonoscillatory scheme (WENO) (Su, Sasaki, and Nakahashi 2013a, 2013b), and the discontinuous Galerkin method (DG) (Ren et al. 2015; Ren and Gu 2016). In this paper, the finite volume second-order-accuracy MUSCL with a three-order interpolation, i.e., the MUSCL4 reconstruction (Garnier et al. 1999), is adopted because it is widely used and is accurate enough compared with other higher-order methods (Garnier et al. 1999; Thornber, Mosedale, and Drikakis 2007). The limiter for shock is not used because it is not necessary for low Mach number flows. The finite volume method,

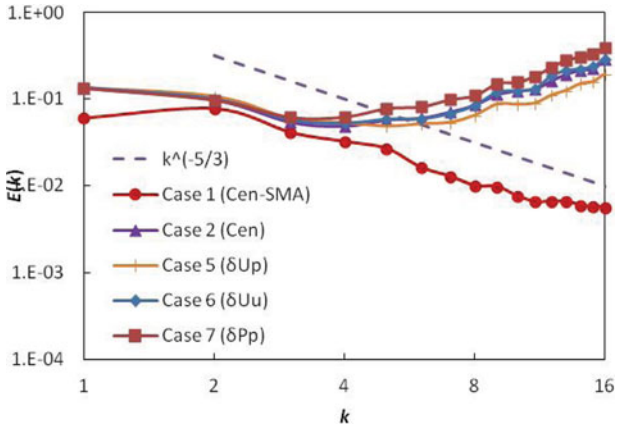

Figure 1. Kinetic energy spectra for Cases 1, 2, 5, 6, and 7 at the 32^3 grid.

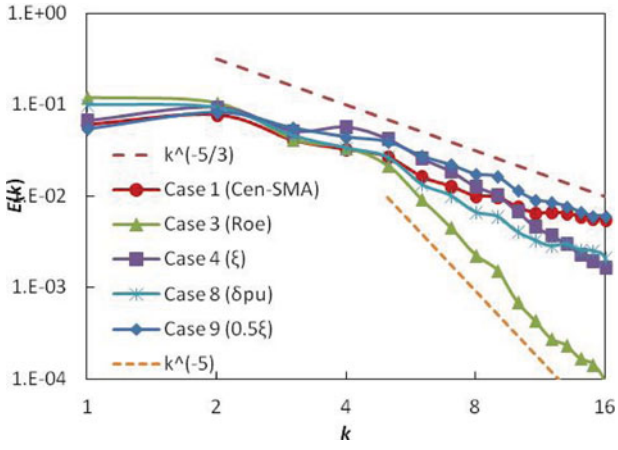

Figure 2. Kinetic energy spectra for Cases 1, 3, 4, 8, and 9 at the 32^3 grid.

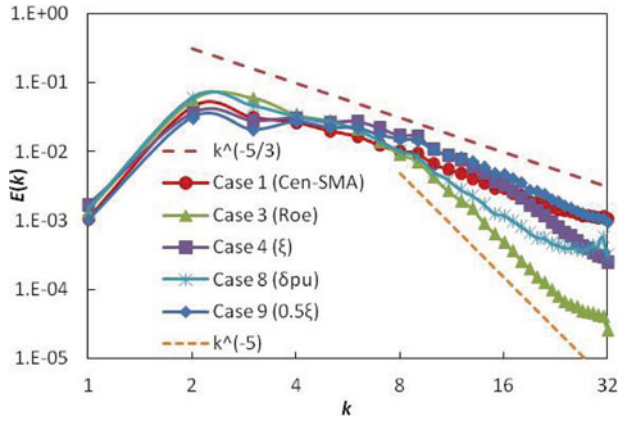

Figure 3. Kinetic energy spectra for Cases 1, 3, 4, 8, and 9 at the 64^3 grid.

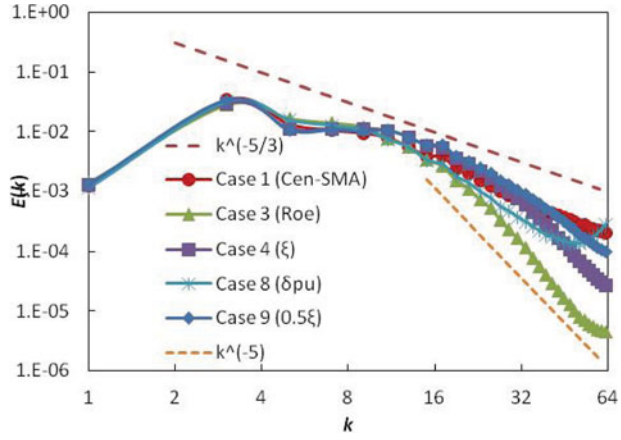

Figure 4. Kinetic energy spectra for Cases 1, 3, 4, 8, and 9 at the 128^3 grid.

and not the finite difference method, is adopted, such as that in reference Thornber, Mosedale, and Drikakis 2007. In this way, the conclusions can be easily extended to the practical CFD computation of engineering problems. For time discretisation, the four-stage Runge–Kutta scheme is adopted.

3.2. LES of homogeneous decaying turbulence

The initial condition for the HDT is set as that in references Samtaney, Pullin, and Kosovic (2001) and Li, Fu, and Ma (2002). The velocity is initially divergence free and is given from the initial energy spectrum $E(k) = Ak^4 \exp(-2k^2/k_0^2)$ with random phase and $k_0 = 2$. All thermodynamic quantities (pressure, density, and temperature) are initially constant. The initial root-mean-square Mach number is 0.2. The spatial mesh resolutions are 32^3, 64^3, and 128^3. The 128^3 grid can obtain satisfactory results, and the 32^3 and 64^3 grids are important in complex practical flows in engineering problems because with limited computational resources, the mesh resolution is usually only equivalent to $32^3 \sim 64^3$ or lower in practice. All simulations for all mesh resolutions are performed up to a period of $t = 5$, which corresponds to approximately seven large-eddy-turnover times because the initial large-eddy-turnover time is approximately 0.71. The definition of large-eddy-turnover time can be found in reference Samtaney, Pullin, and Kosovic (2001). The one-dimensional energy spectrum $E(k)$ is computed by the integration of three-dimensional energy spectrum $E(k_1, k_2, k_3)$ in the spherical shell $k = \sqrt{k_1^2 + k_2^2 + k_3^2}$ in spectrum space, i.e., it is a shell-integrated spectrum.

According to the famous Kolmogorov theory, in the self-similar decay stage, energy is passed down from a low wave number k to a high wave number with $k^{-5/3}$ spectral law in the inertial sub-range. Finally, this energy is dissipated into heat in the dissipative sub-range of sufficiently small length scales by the fluid viscosity. To test the ability of producing important $k^{-5/3}$ sub-ranges, the kinetic energy spectrum is shown in Figures 1–4. As expected, Case 1 (Cen-SMA) produces good results.

Table 2. The velocity structure function of skewness tensor S_3.

	32^3	64^3	128^3
Case 1 (Cen-SMA)	0.21	0.24	0.29
Case 3 (Roe)	0.22	0.33	0.35
Case 4 (ξ)	0.32	0.34	0.38
Case 8 (δp_u)	0.27	0.31	0.34
Case 9 (0.5ξ)	0.26	0.29	0.34

Table 3. The velocity structure function of flatness tensor S_4.

	32^3	64^3	128^3
Case 1 (Cen-SMA)	3.12	3.36	3.48
Case 3 (Roe)	3.20	3.50	3.58
Case 4 (ξ)	3.25	3.44	3.63
Case 8 (δp_u)	3.30	3.57	3.58
Case 9 (0.5ξ)	3.29	3.50	3.73

Table 4. The total integrated kinetic energy k (m^2/s^2).

	32^3	64^3	128^3
Case 1 (Cen-SMA)	0.35	0.39	0.40
Case 3 (Roe)	0.14	0.41	0.39
Case 4 (ξ)	0.13	0.39	0.37
Case 8 (δp_u)	0.36	0.41	0.40
Case 9 (0.5ξ)	0.43	0.38	0.40

For Case 2 (Cen), Case 5 (δU_p), Case 6 (δU_u), and Case 7 (δp_p), convergence fails for all the mesh resolutions. Figure 1 provides the kinetic energy spectrum of the four failed cases before their divergence at the 32^3 grid. As shown in this figure, the energy accumulates in the sub-range of high wave numbers because of the lack of a physical or numerical dissipation mechanism. The result of Case 6 (δU_u) almost overlaps that of Case 2 (Cen); hence, the numerical dissipation of the term δU_u is almost zero. The result of Case 7 (δp_p) indicates that the term δp_p has a small negative dissipation. According to the result of Case 5 (δU_p), the term δU_p having small dissipation is important. Although the term δU_p is not necessary for HDT, it must be maintained in the scheme to suppress the checkerboard problem for practical wall flows; otherwise, the computation will diverge. The indispensable term δU_p fortunately features a negligible dissipation for LES.

Figures 2–4 present the results of Case 3 (Roe), Case 4 (ξ), Case 8 (δp_u), and Case 9 (0.5ξ). Similar conclusions can be obtained for different mesh resolutions. The numerical dissipation of the classical Roe scheme is too large to produce correct $k^{-5/3}$ sub-ranges, which are replaced with approximately k^{-5} sub-ranges for high wave numbers. This problem barely improves with the adoption of higher-order reconstruction methods (Garnier et al. 1999; Thornber, Mosedale, and Drikakis 2007).

The energy spectrum independently produced by the terms ξ and δp_u indicates that each term features a larger dissipation than the correct SGS model. Notably, the behaviour of the term δp_u is not significantly different from that of the term ξ, although it does lead to the non-physical behaviour problem. The reason may be the one-dimensional characteristic of 'homogeneity'. For the one-dimensional computation with the Roe scheme, the non-physical behaviour problem is known to not occur, and the reason is explained by Guillard (2009). For the 64^3 and 128^3 resolutions, however, the energy spectrum of δp_u seems to oscillate at high wave numbers. Considering the possible non-physical behaviour problem for general flows and the non-monotonicity near the cut-off wave number, the term δp_u should be reduced to near zero.

Although the term ξ also produces a large dissipation rate, it should be maintained for computation stability and the improved reduction of dissipation. Simply multiplied by 0.5, the term ξ produces satisfactory energy spectra for all resolutions.

Figure 5 illustrates the iso-surfaces of vorticity, which provide an intuitionistic perspective for observing turbulence eddy and dissipation. Compared with those in Case 1 (Cen-SMA), the vortex cubes with a small space scale corresponding to high wave numbers in Case 3 (Roe) almost disappear because of the large dissipation, and only a few large space-scale vortex tubes are produced. Obviously, Case 4 (ξ) is better than Case 8 (δp_u), which, in turn, is better than Case 3 (Roe). Case 9 (0.5ξ), which is very close to Case 1 (Cen-SMA), appears to be the best.

The velocity structure functions are also important parameters related to the turbulence characteristic, which are defined as follows:

$$S_n = (-1)^n \left\langle \left(\frac{\partial u_i}{\partial x_i} \right)^n \right\rangle \Bigg/ \left\langle \left(\frac{\partial u_i}{\partial x_i} \right)^2 \right\rangle^{\frac{n}{2}}. \tag{28}$$

The third-order structure function ($n = 3$) is the skewness tensor, which is related to enstrophy and non-Gaussian behaviour in HDT. The fourth-order structure function ($n = 4$) is the flatness tensor, which indicates the probability of occurrence of extreme events. As expected, all the results in Tables 2 and 3 increase with an increase in the resolution and fall within a reasonable range. However, the results also indicate that skewness and flatness factors have little relation to the numerical dissipation because of the absence of an obvious rule between cases. Above facts provide some justification of directly adopting the Roe scheme for LES (Garnier et al. 1999; Thornber, Mosedale, and Drikakis 2007).

Tables 4 and 5 give the total integrated kinetic energy $k = \frac{1}{2}\overline{u_i' u_i'}$ and dissipation rate $\varepsilon = \nu \overline{\frac{\partial u_i'}{\partial x_j} \frac{\partial u_i'}{\partial x_j}}$, where the value of ν is $1.711{*}10^{-5}$. For k, all models with all mesh

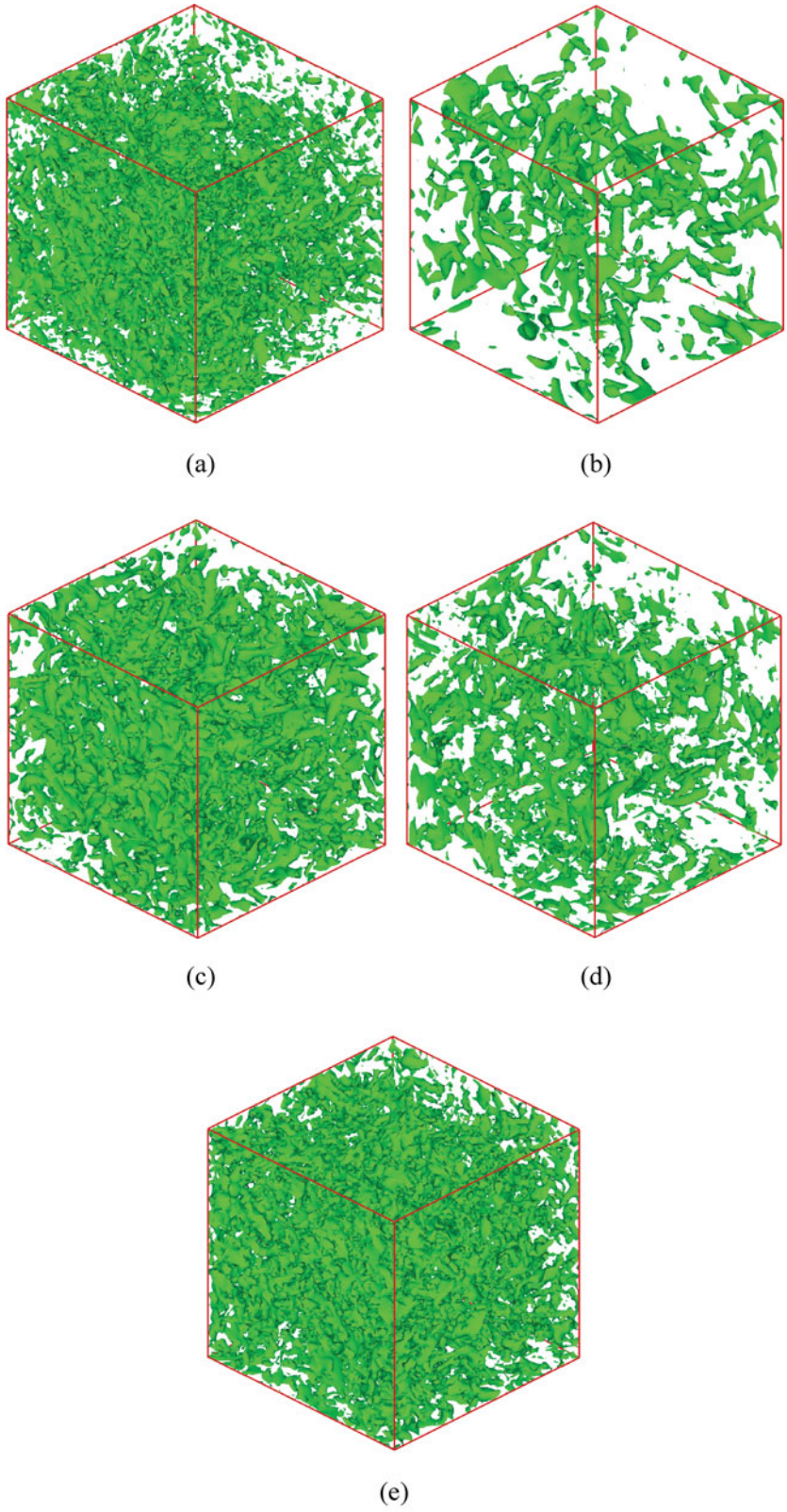

Figure 5. Iso-surfaces of vorticity at $\omega = 8.5$ in the 64^3 grid (a) Case 1 (Cen-SMA), (b) Case 3 (Roe), (c) Case 4 (ξ), (d) Case 8 (δp_u), and (e) Case 9 (0.5ξ).

Table 5. The total integrated dissipation rate ε (10^{-4} m^2/s^3).

	32^3	64^3	128^3
Case 1 (Cen-SMA)	1.91	5.63	14.9
Case 3 (Roe)	0.29	3.46	7.70
Case 4 (ξ)	0.69	5.71	12.6
Case 8 (δp_u)	1.14	3.76	9.61
Case 9 (0.5ξ)	2.66	6.82	14.7

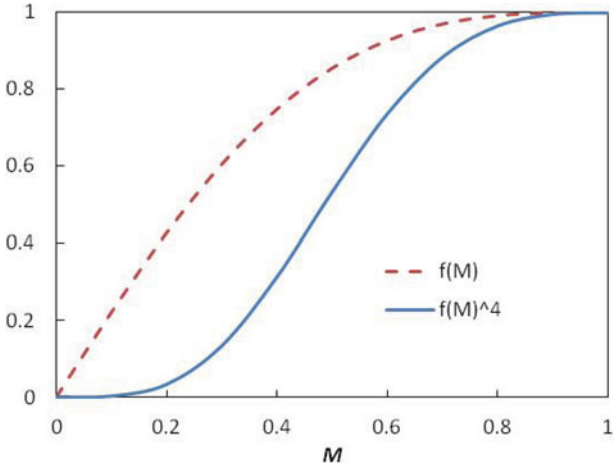

Figure 6. Effect of Mach number on the function.

resolutions obtain approximately value of 0.4, except Case 3 (Roe) and Case 4 (ξ) at the coarse grid 32^3. For ε, the value increases with an increase of grid numbers, because the turbulence is more fully resolved. Case 8 (δp_u), Case 4 (ξ), and especially Case 3 (Roe), obtain obviously smaller values compared with that of Case 1 (Cen-SMA), because the turbulence is overly dissipated by the numerical viscosity, as intuitionisticly shown in Figure 5. Case 9 (0.5ξ) can produce reasonable results similar to that of Case 1 (Cen-SMA).

4. Improvement of the Roe scheme for LES

According to the discussion in Section 3.2, an improved all-speed Roe scheme for LES is proposed as follows:

$$\xi = \alpha_1 \left[1 + f^{\alpha_2}(M)\right] |U|, \tag{29}$$

$$\delta p_u = f^{\alpha_2}(M) \left[|U| - \frac{|U-c| + |U+c|}{2}\right] [U\Delta\rho - \Delta(\rho U)], \tag{30}$$

$$\delta p_p = -\frac{|U-c| - |U+c|}{2} c\beta, \tag{31}$$

$$\delta U_u = \frac{|U-c| - |U+c|}{2\rho c} [U\Delta\rho - \Delta(\rho U)], \tag{32}$$

$$\delta U_p = \frac{1}{\rho}\left(\frac{|U-c| + |U+c|}{2} - |U|\right)\beta. \tag{33}$$

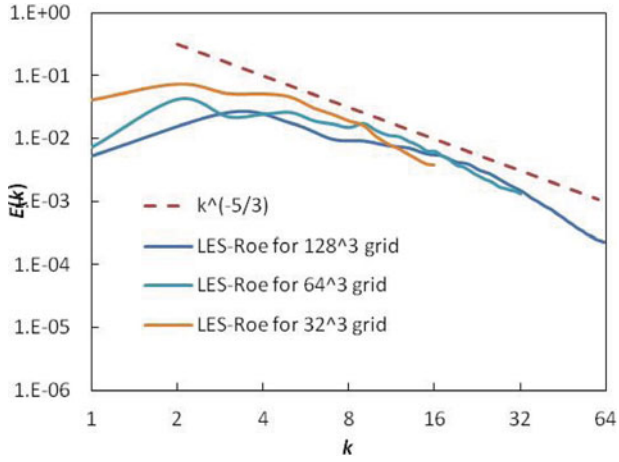

Figure 7. Kinetic energy spectra of the improved Roe scheme for LES at different resolutions.

The differences between the classical Roe scheme and the proposed scheme only lie in the terms ξ and δp_u with the Mach number-related function $f(M)$, i.e.,

$$f(M) = \min\left(M\frac{\sqrt{4 + (1-M^2)^2}}{1+M^2}, 1\right). \tag{34}$$

Equation (34) (Li, Gu, and Xu 2009) is used to smoothen the transonic speed. However, the dissipation in the δp_u term is $\sqrt{5}$ times that in the ξ term when $M \to 0$. Such condition is not important for general low Mach number flows, but it has a significant effect on LES. Therefore, α_2 is chosen as

$$\alpha_2 = 4, \tag{35}$$

which causes δp_u to approach zero in the low Mach number limit (Figure 6).

On the basis of the behaviour of Case 9 (0.5ξ), α_1 is chosen as

$$\alpha_1 = 0.5. \tag{36}$$

Therefore, Equation (29) tends to approach Case 9 (0.5ξ) in the low Mach number limit.

The improved Roe scheme shown in Equations (29)–(36) satisfies the rules (Li and Gu 2013) for overcoming the non-physical behaviour problem, the global cut-off problem, and the checkerboard problem. As expected, the results produced by the improved Roe scheme for LES are very similar to those in Case 9 (0.5ξ). Figure 7 shows that the improved Roe scheme for LES can produce good energy spectra in general for all grid resolutions. Hence, even under coarse resolutions, this scheme can produce satisfactory results for the LES computation of engineering problems.

Table 6. Important factors by the improved Roe scheme.

	32^3	64^3	128^3
S_3	0.30	0.29	0.34
S_4	3.24	3.47	3.71
k (m^2/s^2)	0.40	0.38	0.39
ε (10^{-4} m^2/s^3)	2.71	6.81	14.2

Table 6 shows important factors of the skewness, flatness, the total integrated kinetic energy and dissipation rate, which are obtained by the improved Roe scheme with different mesh resolutions. All results are similar to that of Case 9 (0.5ξ) and are as expected.

5. Conclusions

The Roe scheme in this work is divided into five parts, and the effects of such parts on the LES of HDT are investigated.

(1) The terms δU_u, δp_p, and δU_p have little numerical dissipation that could affect LES. This conclusion is important, especially for the term δU_p, because the checkerboard problem should be suppressed to compute general flows. The term δU_p can be retained in the scheme to achieve computational stability and to ultimately avoid the influence of dissipation.

(2) The terms ξ and δp_u feature a significantly larger numerical dissipation than the SGS model. Given that the term δp_u can be set to zero in the low Mach number limit, we only need to focus on the term ξ. The improvement for ξ should mimic the SGS model to maintain stability. According to the current results, simply multiplying ξ by a coefficient of 0.5 achieves this goal.

Considering all conditions, this work proposes an improved Roe scheme for LES. Under the proposed scheme, LES can be performed with relatively coarse grid resolutions, and usually adopted second-order reconstructions of the finite volume method.

Disclosure statement

No potential conflict of interest was reported by the authors.

Funding

This work is supported by the National Natural Science Foundation of China [project number 51276092].

References

Garnier, E., M. Mossi, P. Sagaut, P. Comte, and M. Deville. 1999. "On the Use of Shock-Capturing Schemes for Large-Eddy Simulation." *Journal of Computational Physics* 153: 273–311.

Grinstein, F.F., L.G. Margolin, and W.J. Rider, eds. 2007. *Implicit Large Eddy Simulation: Computing Turbulent Fluid Dynamics*. New York: Cambridge University Press.

Guillard, H. 2009. "On the Behavior of Upwind Schemes in the Low Mach Number Limit. IV: P0 Approximation on Triangular and Tetrahedral Cells." *Computers & Fluids* 38: 1969–1972.

Guillard, H., and C. Viozat. 1999. "On the Behaviour of Upwind Schemes in the Low Mach Number Limit." *Computers and Fluids* 28: 63–86.

Huang, D.G. 2007. "Preconditioned Dual-Time Procedures and Its Application to Simulating the Flow with Cavitations." *Journal of Computational Physics* 223: 685–689.

Leng, Y., X.L. Li, D.X. Fu, and Y.W. Ma. 2012. "Optimization of the MUSCL Scheme by Dispersion and Dissipation." *Science China Physics, Mechanics & Astronomy* 55: 844–853.

Li, X.L., D.X. Fu, and Y.W. Ma. 2002. "Direct Numerical Simulation of Compressible Isotropic Turbulence." *Science in China A Mathematics* 45: 1452–1460.

Li, X.S. 2014. "Uniform Algorithm for All-Speed Shock-Capturing Schemes." *International Journal of Computational Fluid Dynamics* 28: 329–338.

Li, X.S., and C.W. Gu. 2010. "The Momentum Interpolation Method Based on the Time-Marching Algorithm for All-Speed Flows." *Journal of Computational Physics* 229: 7806–7818.

Li, X.S., and C.W. Gu. 2013. "Mechanism of Roe-type Schemes for All-Speed Flows and Its Application." *Computers and Fluids* 86: 56–70.

Li, X.S., C.W. Gu, and J.Z. Xu. 2009. "Development of Roe-Type Scheme for All-Speed Flows Based on Preconditioning Method." *Computers and Fluids* 38: 810–817.

Li, X.S., J.Z. Xu, and C.W. Gu. 2008. "Preconditioning Method and Engineering Application of Large Eddy Simulation." *Science in China Series G: Physics, Mechanics & Astronomy*, 51: 667–677.

Liou, M.S. 2006. "A Sequel to AUSM, Part II: AUSM+-up for All Speeds." *Journal Computational Physics* 214: 137–170.

Luo, H., and J.D. Baum. 2005. "Extension of Harten-Lax-van Leer Scheme for Flows at All Speeds." *AIAA Journal* 43: 1160–1166.

Park, S.H., J.E. Lee, and J.H. Kwon. 2006. "Preconditioned HLLE Method for Flows at All Mach Numbers." *AIAA Journal* 44: 2645–2653.

Ren, X., and C. Gu. 2016. "Application of a Discontinuous Galerkin Method on the Compressible Flow in the Transonic Axial Compressor." *Applied Thermal Engineering* 93: 707–717.

Ren, X., K. Xu, W. Shyy, and C. Gu. 2015. "A Multi-dimensional High-Order Discontinuous Galerkin Method Based on Gas Kinetic Theory for Viscous Flow Computations." *Journal of Computational Physics* 292: 176–193.

San, O., and K. Kara. 2014. "Numerical Assessments of High-Order Accurate Shock Capturing Schemes: Kelvin–Helmholtz Type Vortical Structures in High-Resolutions." *Computers and Fluids* 89: 254–276.

San, O., and K. Kara. 2015. "Evaluation of Riemann Flux Solvers for WENO Reconstruction Schemes: Kelvin–Helmholtz Instability." *Computers and Fluids* 117: 24–41.

Samtaney, R., D.I. Pullin, and B. Kosovic. 2001. "Direct Numerical Simulation of Decaying Compressible Turbulence and Shocklet Statistics." *Physics of Fluids* 13: 1415–1430.

Shima, E., and K. Kitamura. 2011. "Parameter-Free Simple Low-Dissipation AUSM-family Scheme for All Speeds." *AIAA Journal* 49: 1693–1709.

Su, X.R., D. Sasaki, and K. Nakahashi. 2013a. "Cartesian Mesh with a Novel Hybrid WENO/Meshless Method for Turbulent Flow Calculations." *Computers & Fluids* 84: 69–86.

Su, X.R., D. Sasaki, and K. Nakahashi. 2013b. "On the Efficient Application of Weighted Essentially Nonoscillatory Scheme." *International Journal for Numerical Methods in Fluids* 71: 185–207.

Thornber, B., A. Mosedale, and D. Drikakis. 2007. "On the Implicit Large Eddy Simulation of Homogeneous Decaying Turbulence." *Journal of Computational Physics* 226: 1902–1929.

Turkel, E. 1999. "Preconditioning Techniques in Computational Fluid Dynamics." *Annual Reviews of Fluid Mechanics* 31: 385–416.

Van Leer, B. 1979. "Towards the Ultimate Conservative Difference Scheme. V. A Second-Order Sequel to Godunov's Method." *Journal of Computational Physics* 32: 101–136.

Weiss, J.M., and W.A. Smith. 1995. "Preconditioning Applied to Variable and Constant Density Flows." *AIAA Journal* 33: 2050–2057.